

Energy Recovery Linac: Unique Opportunities to Address Grand Science Challenges

Editors: J.D. Brock, D. Dale, B. Dunham, E. Fontes, S. M. Gruner, G. Hoffstaetter, R. Patterson, J. Ruff

1	Energy Recovery Linac (ERL): a new X-ray research tool.....	1
1.1	ERL: a flexible new linac-based light source	1
1.2	Unique qualities of an ERL.....	1
1.2.1	Round, diffraction-limited source.....	1
1.2.2	High coherent flux	2
1.2.3	High energy X-rays.....	2
1.2.4	High repetition rate, short pulses.....	2
1.2.5	Narrow energy spread.....	3
1.2.6	Many flexible beamlines	3
1.2.7	Opening new horizons.....	3
1.2.8	Technical maturity and competitiveness	4
2	Grand Challenges enabled by the ERL	4
2.1	Grand Challenge: Quantum coherence and control.....	4
2.1.1	Superionic conductivity.....	5
2.1.2	Tracking energy flow in light-harvesting antenna-proteins	5
2.1.3	Dynamic studies in photochemistry.....	5
2.2	Grand Challenge: Designing materials with tailored properties	6
2.2.1	Materials and processes under extreme environments.....	6
2.2.2	Materials discovery via high-pressure processing.....	7
2.3	Grand Challenge: Understanding and controlling collective phenomena	8
2.3.1	Dynamics of phase competition	8
2.3.2	Ferroelectric and multiferroic switching.....	9
2.4	Grand Challenge: Characterize and control matter far from equilibrium	9
2.4.1	Materials processing and multiscale, mesoscale engineered materials.....	10
2.4.2	In-situ and in-operando studies	10
2.5	Cross-cutting Challenge: Statistical laws and complex systems.	11
2.5.1	X-ray Photon Correlation Spectroscopy (XPCS).....	11
2.5.2	New insights into atomic diffusion and stability	11
2.5.3	Dynamics of soft matter and complex fluids.....	12
2.6	Grand Challenge: Imaging and harnessing the nanoscale	13
2.6.1	Imaging structure and reactivity of individual nanoparticles	13
2.6.2	Imaging cells and biomembrane dynamics	14
3	ERL Technology Readiness	15
3.1	Photoinjector	15
3.2	Superconducting RF Linac.....	16
3.3	Remaining R&D.....	16
4	Table 1: Parameters used to compare third and fourth generation X-ray sources	17
5	References.....	18

1 Energy Recovery Linac (ERL): a new X-ray research tool

1.1 ERL: a flexible new linac-based light source

The grand science challenges of our age require new research tools, including a complement of forefront light sources, to characterize atomic-scale structure, function and dynamics of time-varying and non-equilibrium systems. Two overarching roles—and challenges—for next generation light sources are (1) to achieve temporal resolution necessary to follow the dynamics of electrons, spins, atoms and chemical reactions down to the femtosecond time scale, and at the same time (2) to enable spectroscopic and structural imaging of nano objects or nanoscale regions of inhomogeneous (and possibly non-crystalline) materials [1]. These dual advances in state-of-the-art observational techniques will drive a paradigm shift to an era of “control science”.

An Energy Recovery Linac (ERL) would be a premier X-ray light source to achieve these goals. Like other linac-based sources, the exquisite quality of the injected electrons transfers directly to the photon beams, producing X-rays limited in the transverse plane only by the fundamental wave nature of light. These intense beams can focus to (sub)-nanometer beam waists while maintaining precise collimation, high photon energy, tunable polarization [2-4] and short pulse lengths. Such beams will enable three-dimensional, real-time characterization of atomic, electronic and molecular structure, and chemical composition and dynamics, in specimens ranging from nanocrystals to macroscopic, non-periodic and heterogeneous systems.

An ERL differs from other linac-based light sources in that it supports high repetition rate and high time-averaged currents. Together with narrow energy spread and short pulse lengths, this unique combination of electron beam qualities lets an ERL operate a high repetition rate oscillator-based FEL, and also creates new capabilities to study pump-probe relaxation dynamics on femtosecond timescales in the critical “small perturbation” regime. To avoid the enormous power demands of a single-pass machine, an ERL recovers the energy from previously accelerated electrons to accelerate new ones. As a result, an ERL light source is a unique and efficient tool to create high energy X-rays with a flexible, quasi-continuous bunch structure, small round beams, short, tunable pulse lengths, and very high transverse coherence. Together, these photon characteristics promise a unique program of transformational science.

1.2 Unique qualities of an ERL

Laboratories that have developed ERL designs include KEK, Cornell and APS using 3, 5 and 7 GeV electron beams respectively [5-7]. While differing beam energies produce different X-ray spectra, all provide the same general features. The following discussion refers to the 5 GeV Cornell design, which is representative. The parameters are shown in Table 1. ERLs are very flexible, and offer several operating modes, including “High Flux”, “High Coherence”, and “Short Pulse”, as well as a mode in which it drives an “XFEL” or “XFEL Oscillator.” Unless otherwise noted, the applications below refer to the “High Flux” mode.

1.2.1 Round, diffraction-limited source

ERL electron beams are round, with transverse emittance as low as 8 pm in both directions, yielding hard X-ray beams of superlative spectral brightness. Spectral brightness is shown in Fig. 1. The small, round source will optimize two-dimensional focusing geometries, enabling cutting-edge nanometer-resolution studies of structure and spectroscopy via scanning probe methods.

1.2.2 High coherent flux

One consequence of ERL's superlative spectral brightness is the production of high coherent flux photon beams (Fig. 1). With 100 mA electron current and a 25 m undulator, an ERL will deliver coherent flux in excess of 10^{14} ph/s/0.1% at 10 keV. This high coherent flux will enable nanometer resolution studies of the structure of crystalline as well as non-crystalline materials via coherent scattering methods, as well as studies of fluctuation dynamics with greatly improved time resolution over what can be achieved at third generation sources.

1.2.3 High energy X-rays

While an ERL can produce low-energy X-rays, it also produces higher-energy beams at 100 keV (or more) where wavelengths are well-matched to interatomic distances. High-energy X-rays are penetrating, so they probe deeply buried interfaces and structures. For example, at 60 keV, the transmission of X-rays through 2 cm of water is 65%, a factor of 15,000 greater than at 10 keV. Moreover, at high energy, the curvature of the Ewald sphere is such that large portions of reciprocal space can be sampled by an area detector; this allows for rapid data collection for time-resolved experiments. A 5 GeV ERL provides as much coherent flux at 30-40 keV as third generation sources provide at 10 keV, enabling new experiments in extreme environments (*i.e.* diamond-anvil cells) or in-operando devices.

1.2.4 High repetition rate, short pulses

While the time-average flux, spectral brightness, and transverse coherence of an ERL are comparable to that of an XFEL, the time structure is very different, delivering a steady stream of pulses separated by about 1 ns. This high rep-rate beam structure has much lower peak electric field amplitudes, greatly reducing specimen damage. The natural pulse length of an ERL is 2 ps, with compression possible to 50 fs. The short pulses and high average coherent flux of an ERL will enable a new class of "tickle and probe" experiments where the sample is repeatedly probed inducing much less radiation damage than an XFEL. Together, the high coherent flux and qua-

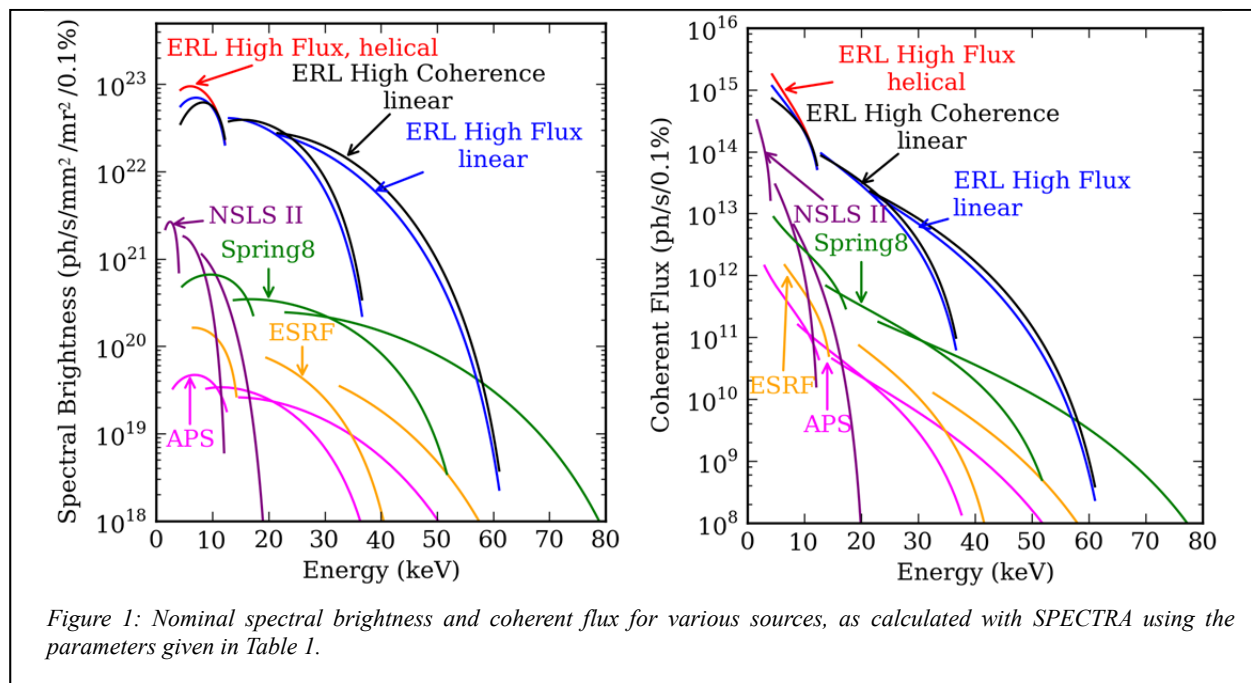


Figure 1: Nominal spectral brightness and coherent flux for various sources, as calculated with SPECTRA using the parameters given in Table 1.

si-continuous time structure are superb for studies of dynamics.

1.2.5 Narrow energy spread

The electron beam in an ERL has very narrow energy spread ($\sim 0.02\%$). This, together with the diffraction-limited emittance, allows an ERL to utilize very long undulators to produce X-ray beams with very narrow energy bandwidths (undulator harmonic energy spread $\sim 10^{-4}$). These undulators will power beamlines for spectroscopies (e.g. inelastic X-ray scattering) without the complexities (heat loading, wavefront spoiling, etc.) of using an X-ray monochromator to achieve high energy resolution from a beam with larger energy spread (typical for storage ring sources) [8].

1.2.6 Many flexible beamlines

Like a storage ring, an ERL can serve a large number of beamlines operating in parallel [7,9]. Moreover, because an ERL is a single pass machine, these beamlines may operate with individualized beam-size and beam-divergence (Twiss) parameters, tuned to the scientific needs of that particular beamline or end station. These parameters can be optimized for a given beamline and undulator length to yield the smallest source size or best collimation.

Having a full complement of beamlines ensures that an ERL light source will have broad, visible scientific impact, and a lively program to develop new scientific techniques and applications. These features are particularly attractive in today's restricted-budget research environment

1.2.7 Opening new horizons

An ERL could also drive a versatile XFEL source with high repetition rates or a revolutionary new source like the X-ray Free Electron Oscillator (XFEL) [10], a tunable X-ray resonant cavity, which produces Fourier transform-limited X-ray pulses with a coherent intensity of over 10^9 X-rays per pulse. This flux is much higher than typical undulator radiation pulses, but three orders of magnitude less than from an XFEL, thereby reducing sample damage impacts. The pulses from an XFEL would have MHz repetition rates and extremely high energy resolution [10,11] (Fig. 2), 10^4 times narrower than that of an XFEL. These beams are ideally suited to study thermal (1 meV) excitations that govern transport properties in solids, as well as technologically important phenomena like superconductivity. For the first time, X-ray sources would have all the properties one expects from a laser and could yield new applications and fields of scientific study, such as non-linear X-ray optical processes, multi-photon correlation techniques applied to electronic states and wave packets, extension of transient grating methods to atomic length-scales, and X-ray standing wave studies of non-crystalline materials. And, lastly, new horizons may be opened by using ERL technology to upgrade existing third generation storage rings to fourth-generation sources.

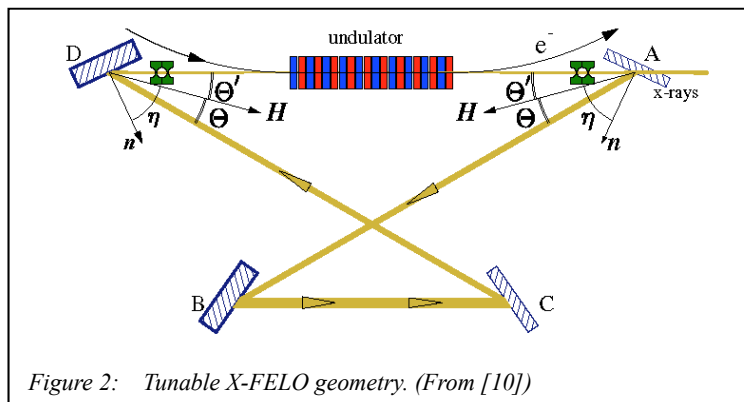


Figure 2: Tunable X-FELO geometry. (From [10])

1.2.8 Technical maturity and competitiveness

The guiding concept for an ERL source was originated by Tigner in 1965 [12]. For many years, the DOE has supported a low-energy ERL at Jefferson Laboratory to drive the world's highest-power tunable infrared and VUV laser. Studies for an ERL light source have also been done at APS [13]. KEK in Japan is building a low-energy compact ERL, and is planning to build a full-scale 3 GeV ERL X-ray source [5]. England, Germany and China have also expressed interest [14]. Over the past decade, an NSF-supported effort at Cornell has succeeded in designing, fabricating, and demonstrating the technologies needed to create a high-energy ERL light source: a prototype minimum phase space injector and superconducting accelerator cavities. **All the necessary technology milestones have been achieved or proven through validated models [7,15,16].** These results are discussed in more detail in Section 3.

2 Grand Challenges enabled by the ERL

This section explores the potential of an ERL to address grand science challenges identified by prior BES advisory committees. Example experiments and applications are drawn from topics identified during international workshops in 2006 and 2011 [17-19]. Details are available in "Science with an Energy Recovery Linac" [20].

2.1 Grand Challenge: Quantum coherence and control

X-rays have played a critical role in developing our fundamental understanding of the atomic-scale structure of matter. Our next challenges are to understand function and to direct and control it in order to create new opportunities in areas like photochemistry, catalysis, molecular biology, among others. How does the potential energy landscape or electronic structure constrain function? How can these be modified to augment function, or enable entirely new functionality? Can such studies provide insights into quantum coherence to enable control on the level of electrons?

ERLs offer exciting opportunities to understand both reversible and metastable dynamical processes in solid-state systems, and for influencing those processes. Most physical systems need only mild pumping (tickling), perhaps inducing 0.1% changes in physical properties. These small changes have to be measured with at least a 0.01% noise floor - hence the need for high repetition rates. The ERL will provide flux increases of 10^4 relative to existing state-of-the-art slicing and low-alpha sources. The combination of high repetition rate and extremely high timing stability (virtually no timing jitter) makes the ERL an ideal source for ultra-fast dynamics studies. Photon beams from an ERL would be ideally suited to "tickle-probe" or "pump-probe" dynamical studies because of its short pulses of more moderate intensity at very high repetition rates (1.3 GHz).

In the past, high power pump lasers used for spectroscopies are typically limited to operating at repetition rates less than 1 kHz. With the advent of intense fiber-based 0.1-10 MHz laser systems with 1-10 μ J pulse energy in the visible domain, studies employing higher frequency pumps can take advantage of the much larger X-ray repetition rates at an ERL. High repetition-rate pump-probe experiments on atomic length- and time-scales open a largely unexplored regime of experimental phase space. Moreover, experimenters may utilize several ERL X-ray probe pulses per pump cycle to make a "movie" of the time evolution.

2.1.1 Superionic conductivity

The dynamics associated with superionic materials are important for next generation energy capture and storage applications. These compounds exhibit ionic conductivities of order $1 \text{ } \Omega^{-1} \text{ cm}^{-1}$ and incorporate one ionic species moving with liquid-like diffusivity through an otherwise fixed crystalline lattice [21]. Scientists need to understand the response of lattice motion to an ion, but this requires the ability to push ions in well-defined directions before coupling to atomic-scale X-ray diffraction probes. This can be enabled through THz excitation resonant with the ionic plasmon mode of the superionic state. This work could potentially have a large impact on developing and understanding factors limiting the performance of electrochemical devices.

2.1.2 Tracking energy flow in light-harvesting antenna-proteins

Biomimetic research attempts to copy or incorporate biological processes or components into engineered materials, processes, and devices. Light-harvesting antenna proteins collect solar energy and efficiently transport resulting electron-hole pairs to photosynthetic reaction centers where chemistry occurs. The ability of light harvesting molecules to efficiently guide energy makes them intriguing candidates in nanofabricated photonic devices.

In individual proteins, electronic excitations travel up to 50 nm and are thought to last hundreds of picoseconds. Nanofabricated arrays of antenna proteins have been used to observe long-range energy migration in bioengineered, closely packed arrays of LH2 antenna complexes [22]. The experiments showed evidence of excitonic transport over microns, a distance much larger than required in the parent bacterial system. These results demonstrate the potential to use natural antennas from photosynthetic organisms in hybrid systems for long-range energy propagation. Bioengineering may have a profound impact on strategies to harvest and transport solar energy in devices for sustainable energy production.

Temporal and spatial mapping of charge migration and protein solvation could be resolved on ps time- and 10 nm length-scales using either X-ray Emission Spectroscopy (XES) or Resonant Inelastic X-ray Scattering (RIXS) following an optical excitation. RIXS offers combined sensitivity to unoccupied and occupied electronic structure, so it can distinguish protein response to electron transfer. Measurements of this type, requiring X-ray energy tunability, few nm spot size, and high repetition sub-ps pulses will be enabled by the ultra-high brightness of ERL sources.

2.1.3 Dynamic studies in photochemistry

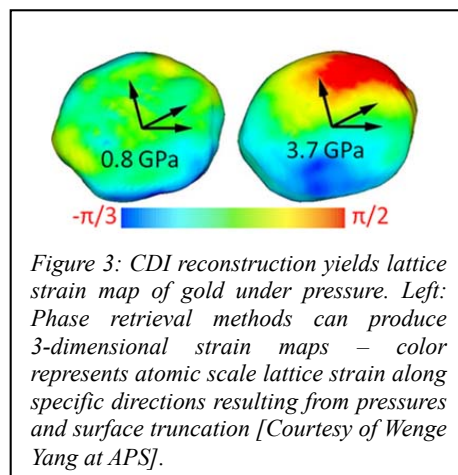
Ultrafast laser spectroscopies uncover mechanisms for charge transfer and spin switching. However, the elementary steps of photochemical activity, with intermediates limited to the first few hundreds of femtoseconds following photo-excitation, remain elusive. Understanding such phenomena will have direct influence on chemical applications, improved dye-sensitized solar cells and photo-catalytic activity, and the development of other functional materials.

Time-resolved X-ray spectroscopy and scattering have the potential to provide both local and global structural dynamics information down to the molecular time scale of femtoseconds. Recently, researchers have taken the first steps towards structural dynamics studies of a multi-chromophoric Ru-Co transition metal complex with its potential for catalytic functions [23]. Combining XES and X-ray Raman Spectroscopy (XRS) has the potential to deliver a quasi-motion-movie of the entire process involving nuclear and electronic rearrangements. The combination of ultrafast XAS and XRS on transition metal complexes with realistic photochemistry is the first important and necessary step towards the understanding catalytic complexes.

2.2 Grand Challenge: Designing materials with tailored properties

Every technological application is constrained by intrinsic bulk properties, the properties of surfaces and interfaces, and/or the response of these systems to local environments. Developing new materials is typically a slow and painstaking process. Only a tiny fraction of all the possible chemical compounds have been prepared and characterized. The parameter-space is simply breathtaking: 90 elements could produce over 700,000 ternary phase diagrams, each of which would need to be explored as a function of temperature (for example). To make progress scientists need to develop efficient methods to design new forms of matter with properties tailored for human applications. This requires developing a thorough understanding of bulk and surface properties, how particular local environments influence things like durability and corrosion resistance, mechanical failure, catalytic activity, biocompatibility, and how all of these properties and responses change as particle sizes shrink to the nanoscale.

Meeting this grand challenge will require not only the average structure provided by standard crystallography, but details of non-periodic structures as well. What happens at surfaces and interfaces? How do grains in structural materials respond to local stresses? How do materials respond to extreme environments, like high temperature, high pressure, under working electrochemical conditions? Imaging techniques based on transversely coherent sources will be a critical probe. An ERL is an ideal source for interrogating unique samples. The high time-averaged spectral brightness and coherent flux enable coherent imaging techniques and nanoprobe with orders-of-magnitude increases in spatial or temporal resolution and throughput not achievable at third-generation sources. The relatively moderate peak flux allows sample to be probed repeatedly without perturbation, required for tomographic imaging or ptychographic imaging of extended samples. The coherent flux at higher energies will enable high-resolution imaging of buried materials and interfaces.



2.2.1 Materials and processes under extreme environments

High pressure (HP) studies explore physical properties including phonon, electron and atomic structures, as well as chemical properties such as interatomic forces, bonding, reactivity and kinetics. Changes in pressure and temperature cause materials to cross barriers between insulator-conductor-superconductor, molecular and extended frameworks, and from inert to vigorously reactive compounds. With theory and computation, HP experiments provide understanding of physical and chemical properties of materials and mechanisms of formation.

Extreme condition studies, begun at 3rd generation sources, are almost always photon starved and many regimes and questions remain unexplored over a wide range of pressures, temperatures, and time scales. Static compression studies, even on strongly scattering materials, are limited to maximum a pressure of 300 GPa; in low-Z systems the maximum practical working pressure is below 100 GPa. Achieving higher pressures requires further shrinking already tiny sample volumes. ERL hard X-ray beams can be focused to incredibly small sample volumes, greatly enhancing the signal for studies in extreme environments. An ERL will also generate short pulses for time-resolved dynamic experiments under extreme pressure and

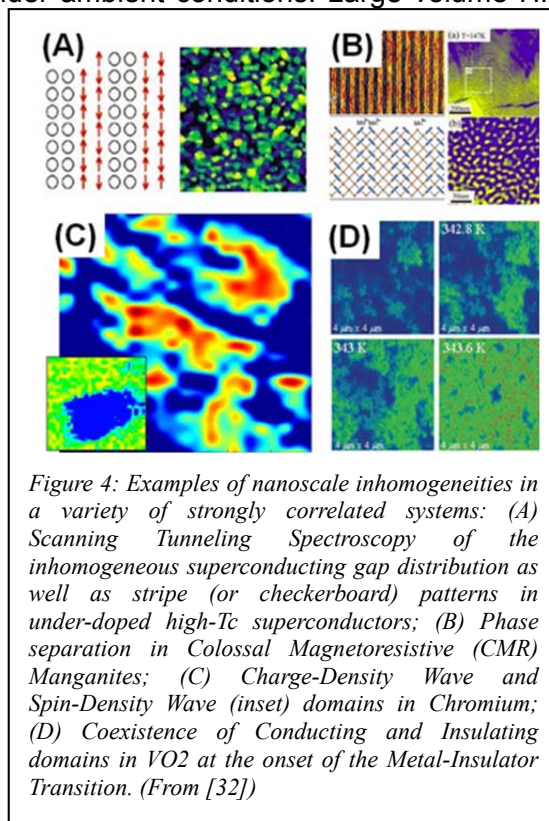
temperature. Dynamic compression provides access to the most extreme conditions, but only for very short periods of time. The ERL time structure will provide unique opportunities for such studies, and could enable structural studies which to date have not been possible.

Coherent diffraction imaging (CDI) of nanoscale strain will gain wide application for nanomaterials under extreme pressure and temperature and during deformation or chemical processing. Such X-ray methods are especially suited for *in-situ* measurements. Nanoscale materials often exhibit unusual strength, so it is important to examine them under stresses that lead to breakdown (Fig. 3). X-ray CDI can also be used to study pattern formation in materials synthesis, for example to understand growth limitations associated with self-assembly in the presence of surfactants. An ERL will greatly improve upon these capabilities, delivering beam with unprecedented transverse coherence and extending the useful energy range into high-energy, enabling 3D imaging of both the sample and strain distribution as a function of pressure.

2.2.2 Materials discovery via high-pressure processing

HP also promotes synthesis of novel functional materials, oftentimes suppressing decomposition of reactants and products that occur under ambient conditions. Large volume HP apparatus produce desirable products unavailable by ambient pressure synthesis, most famously the superhard diamond and c-BN used in industrial composites. The sheer number of phenomena discovered, most without prior recourse to theory as a guide, suggests a wealth of untapped novel materials, potentially with transformative properties. Theory continues to generate exciting possibilities for synthesis in areas as diverse as super-hard materials, superconductivity and photo-catalysis. Despite its great promise, HP synthesis is laborious, and compared to high temperature synthesis, is grossly underutilized - especially in the discovery stage where many experiments need to be optimized. Further, recovery of non-equilibrium phases, which provide valuable insights into transformational properties, is not always possible.

Additional infrastructure is needed to explore the pressure-temperature-composition space to identify new transformational materials. Dramatically increasing the amount of information derived from a single HP loading in the LVHPD or DAC would involve combining theory with the capabilities of ERLs for diffraction, imaging, and spectroscopy, to study multiple phases and their behavior *in-situ* processing (*i.e.* during compression, heating, quenching, etc.). Theory-directed *in-situ*, combinatorial approaches will dramatically shorten the discovery cycle as well as enhance efforts to identify new materials using established approaches.



2.3 Grand Challenge: Understanding and controlling collective phenomena

Four decades ago, Anderson famously wrote “More is different” – identifying scale and complexity as fundamental unsolved problems in modern science [24]. Intervening years have underscored the validity of this claim. Increasingly, we look at strongly correlated electronic states, which emerge collectively in materials, for solutions to pressing energy and engineering challenges. Unconventional superconductors, multiferroics, thermoelectrics, and magnetoresistors promise transformative new technologies. Exotic new electronic order parameters with “nematic”, “hidden”, and “topological” character have been proposed, but conclusive observation requires a new generation of experimental precision. Understanding ordered phases and elementary excitations in complex oxides, how they compete and coexist, and how they respond to varying external fields, are the next steps towards engineering control of electron correlations. Critically, this must be achieved over a large range of length and time scales, from the atomic to the macroscopic, from femtoseconds to hours.

The highly tunable beams generated by an ERL, particularly in concert with novel Delta-type undulators [25] inspired by the small, round ERL source, will be transformational to correlated electron physics studies. These undulators exploit small round ERL beams to create fully and independently tunable incident energy and incident polarization, at a level that has never been achieved at 3rd generation sources. For resonant/anomalous studies of spin and orbital magnetism or time reversal symmetry breaking in superconductors, as well as for resonant inelastic X-ray scattering (RIXS), fully tunable polarization is a giant leap forward. Likewise, the high coherent flux and nanoscale incident beams enable unprecedented detailed studies of electronic inhomogeneity in materials, both via speckle and scanning nanoprobe techniques.

2.3.1 Dynamics of phase competition

Strongly correlated systems often involve competition between spin, charge, orbital and lattice degrees of freedom, resulting in spontaneous emergence of nanoscale inhomogeneities (Fig. 4) [26-32]. Stripe phases and phase coexistence observed in underdoped high-T_c superconductors and colossal magnetoresistive (CMR) manganese oxides are evocative examples. Understanding multiphase competition requires coupling to charge, spin, orbital and lattice order parameters simultaneously, with spatial resolution ranging from nanometers to microns. It is not yet clear whether the domain formation, for example in CMR manganites, is always entirely due to phase competition, or if the crystalline imperfections strongly influence formation of textured patterns. X-ray microdiffraction is unique in providing detailed nanoscale distribution of both crystalline imperfections (strain, defects) and the structure of charge-, orbital- or spin-ordered domains.

The development of lensless imaging based on phase-retrieval algorithms makes it possible to take advantage of the highly coherent X-ray beams from an ERL facility to probe spin, charge, lattice and orbital degrees of freedom in correlated electron systems with nanometer-scale resolution. The high coherent flux produced by an ERL will make it possible to study the dynamics of this competition at timescales 100 to even 10,000 times faster than at current 3rd generation sources. Imaging structures will be at least 100 times faster, making nanometer-scale resolution routinely accessible.

2.3.2 Ferroelectric and multiferroic switching

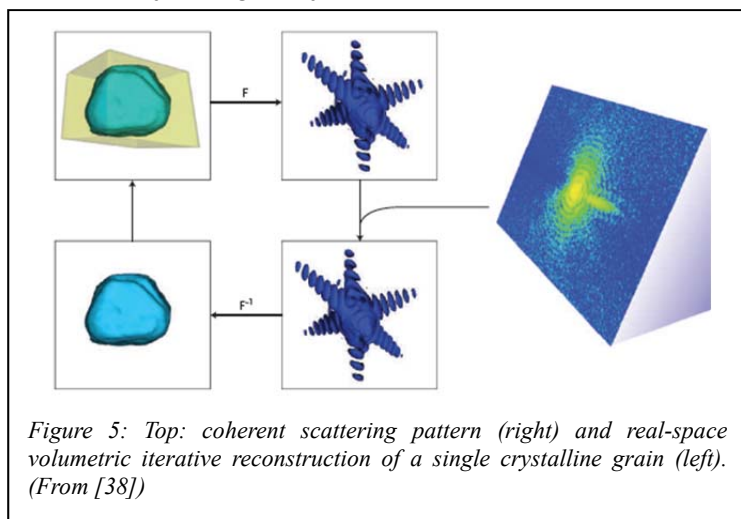
In order to understand speed limits on ferroelectric/multiferroic switching (*i.e.* for next generation information storage applications), scientists need to drive (in resonance) soft modes that underlie ferroelectricity by applying quasi-half-cycle pulses in optical geometries. Efficient ferroelectric switching could be obtained by coherent synchronization of shaped THz pulses with anharmonic oscillations [33]. It may also be possible to bypass the energy barrier between up/down domains using polarization of THz pulse with respect to polarization of films. The short pulses of the ERL will enable generating THz sequences directly from the electron beam, which would enable phase-synchronous pump pulses without timing jitter. In this experiment scientists could simultaneously apply X-ray scattering techniques from Bragg peaks as well as diffuse scattering in order to visualize the atomic-scale response.

2.4 Grand Challenge: Characterize and control matter far from equilibrium

Although X-rays have been used to solve the periodic structure of crystalline materials for more than 100 years, many important materials are not periodic (*i.e.* glasses, polymers). Even in crystalline materials, many important and useful properties are strongly influenced by deviations from long-range periodic order: *e.g.* surfaces, grain boundaries, impurities and dislocations. Adding complexity, most structures are not static but evolve during process or function. Many current technologies and applications are constrained by these effects. Consequently, there is a growing emphasis to understand non-periodic structures and how they evolve over time.

New coherent X-ray methods such as X-ray holography [34-36] and coherent diffraction imaging (CDI) [37-40] have the potential to address these challenges [41], allowing structural solutions to non-periodic systems (see Fig. 5) [39,42,43]. Furthermore, due to the nature of their interaction with matter, hard X-rays are uniquely suited to study thick samples and samples in captive or harsh environmental conditions, including operating devices. Also, coherent imaging techniques can be combined with other rich spectroscopies made possible with X-rays, allowing elemental sensitivity via resonant scattering, trace element sensitivity via X-ray fluorescence, and imaging distributions of chemical states via X-ray absorption near-edge spectroscopy.

Most of these techniques are currently limited by available coherent X-ray flux. An ERL delivers photon beams with orders of magnitude higher coherent flux than current storage rings [41], and with quasi-continuous time structure providing capabilities unique and complementary to XFELs. Three-dimensional coherent scattering measurements taking hours could take a few seconds. Studies of the evolution of non-periodic structures under operating conditions will revolutionize the way we approach materials design, synthesis, and processing, which in turn will have far-reaching and profoundly positive effects on society.



2.4.1 *Materials processing and multiscale, mesoscale engineered materials*

Most materials are polycrystalline and understanding how the size, structure, and interfaces between crystalline grains control material properties is one of the grand challenges in materials science. This subject also has important practical applications, such as crack propagation, fatigue and failure in common metals used for bridges and aircraft parts [44]. Addressing this challenge requires detailed, 3D spatially-resolved measurements of deformation and microstructure on length scales of a typical grain. Submicron spatial resolution of grains and interfaces would enable scientists to explain strength and failure modes of metals and ceramics, ionic diffusion in fuel cell electrodes, dynamical properties of alloys, etc. As grains shrink, the relative contribution of surface to overall free energy becomes increasingly important, which is why nanocrystalline materials often have very different properties than materials of the same composition with micron-sized grains.

Coherent diffraction imaging (CDI) in the Bragg geometry offers a unique view of mechanisms of grain growth on the nanoscale [38,45]. With sensitivity to strain and orientation, scientists could map individual grains of a polycrystalline sample with nanometer resolution to record 3D strain from finite size and boundary effects. CDI is limited by coherent flux; a 3D CDI pattern with 20 nm resolution currently takes hours to record at the APS. With an inverse fourth power relationship between resolution and flux, at an ERL the same pattern with 2 nm resolution could be recorded in a few hours, or a 20 nm resolution pattern recorded in a few seconds. CDI could also be performed at considerably higher X-ray energies, where current beamlines suffer from very short coherence lengths, allowing access to higher order Bragg peaks to interrogate thicker and denser materials, including experiments inside diamond anvil cells.

2.4.2 *In-situ and in-operando studies*

3D micro- and nanodiffraction mapping is an emerging area of electron microscopy and synchrotron science, providing quantitative information on how small sample volumes respond to local environments and external forces. Because the behavior of most material systems is dominated by local heterogeneities and defects, the ability to study small “local” volumes represents a transformative advance over ensemble average information and is certain to revolutionize our understanding of materials. X-ray methods interrogate local strain, structure and texture in 3D volumes in a nondestructive way and, if fast enough, can follow real materials responding to applied loads, heating, and other processing conditions. Detailed information of this sort has never been available.

An ERL will have huge impacts on techniques like differential aperture microscopy (DAM) or X-ray diffraction contrast tomography (DCT) [46,47] (Fig. 6), to name a few. First, high intensity focused beams will accelerate measurements, enabling either novel scanning modes or time resolution for evolving systems. Second, small, round beam sizes can create microscopes with advanced achromatic optics (producing diffraction-limited beams) and longer working distances. For example, fly-scan methods with fast X-ray detectors will make it possible to map 2×10^6 volume elements/hour, enabling unprecedented visualization of materials structure and behavior

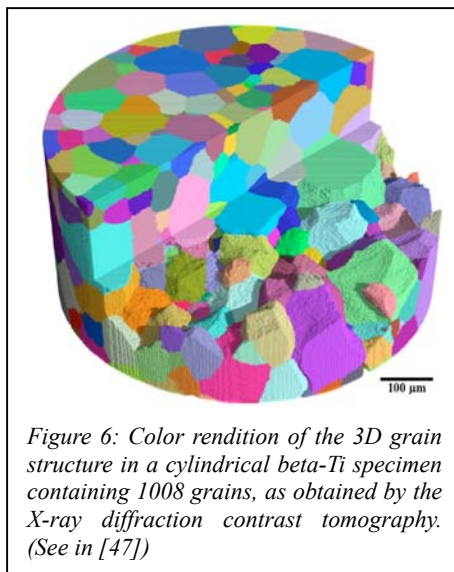
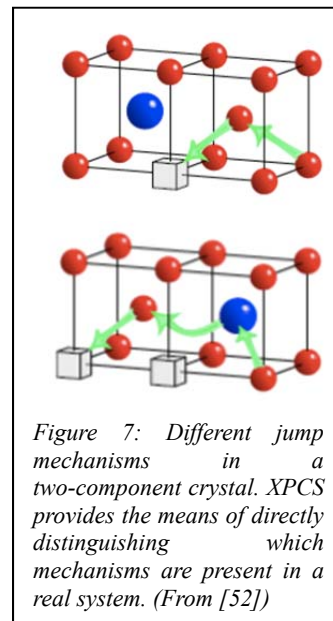


Figure 6: Color rendition of the 3D grain structure in a cylindrical beta-Ti specimen containing 1008 grains, as obtained by the X-ray diffraction contrast tomography. (See in [47])

in minutes, instead of days. In addition, while spatial resolution of 2 nm has been achieved today, the brilliance of ERLs will extend DAM into the coherent regime move spatial resolution to far smaller length scales.

2.5 Cross-cutting Challenge: Statistical laws and complex systems.

Characterizing, understanding and manipulating the dynamical structure of matter at the nanoscale are emerging and critical science frontiers in the 21st century. This frontier covers a wide range of materials, technological demands, and scientific disciplines. For example, the time evolution of microstructures formed under nonequilibrium conditions – conditions common during synthesis of most industrialized materials - is notoriously difficult to study, yet strongly influences (or dominates) the physical and mechanical properties of materials such as tensile strength and failure, chemical reactivity and magnetic coercivity. How magnetic data storage media set or forget previous states, and the dynamics of hysteresis loops, are all features that can be understood by correlating diffraction features (speckle patterns) over time. The ERL will address challenges to obtaining information in such systems in a non-destructive way, over a very wide range of timescales (femtoseconds to seconds), on systems in various states of equilibrium, and with varying (but usually opaque) macroscopic densities.



2.5.1 X-ray Photon Correlation Spectroscopy (XPCS)

A wealth of information can be learned by carefully examining time-dependent intensity profiles, called speckle, resulting from illumination with coherent X-ray beams. Since X-rays probe real-space periodicities, time varying speckle patterns provides a near-unique probe of *time* scale of fluctuations at particular, selectable *length* scales. To date, potential applications of XPCS have been limited by the flux of coherent hard X-ray beams.

ERLs allow XPCS to open new avenues of research into the dynamical structure of materials. The signal-to-noise ratio in XPCS for ergodic processes scales as the square of source brilliance, a 100-fold increase in coherent flux at high energies lets an ERL access time scales 10^4 times faster [41], pushing the frontier of detectable fluctuations to the nanosecond. The short pulse length (below 2 picoseconds) of the ERL allows fast exposures, and the high 1.3 GHz repetition rate allows time averaging to minimize pulse shot noise. The quasi-continuous bunch structure of ERL pushes the time domain towards nanosecond resolution, and the linac-based injection cycle avoids “gaps,” or missing pulses, characteristic of storage rings or low rep-rate XFELs [41]. All told, there is an important gap in the accessible experimental time domain (6 orders of magnitude $Q \approx 1 \text{ \AA}^{-1}$) that ERL will fill, taking great advantage of fast area detectors on the horizon with small pixels and fast image readout. Areas ripe for study include systems far from equilibrium such as glasses and materials under shear and flow, complex fluids such as polymers and colloidal suspensions, moving domain walls, defects in crystals, and proteins in solution.

2.5.2 New insights into atomic diffusion and stability

Although atomic diffusion is critical to materials synthesis and stability, and thus dictates the behavior of much of the material world, it is extraordinarily difficult to measure. In addition to

neutron [48] and helium probes [49] and field ion microscopy [50], 3rd generation X-ray sources have enabled new kinds of diffusion studies with XPCS; however, a very limited number of model systems have profited and scope is often limited to either heavy elements or high temperatures.

An ERL would significantly expand the range of materials systems studied and types of environmental conditions accessible. With much higher brightness and coherent flux, ERLs make it possible to use XPCS to study diffusion in compound materials systems with atomic numbers close to each other, such as technologically important heavy-duty alloys of Ti-Al or Fe-Co-Ni alloys. An entirely new avenue of potential research will be studying motion of light interstitials (hydrogen, lithium or carbon) in host lattices. Although small atoms diffusing through lattices give little signal, fluctuating lattice distortions caused by interstitial diffusion could be recorded by XPCS [51] (Fig. 7). Heroic demonstration experiments at ESRF [52] employed count rates of 1 count per 10 minutes per pixel! An ERL would increase count rates by upwards of 3 orders of magnitude, rendering such measurements routine, and allow different jump mechanisms to be distinguished. XPCS on light elements could have immediate impact on studies of hydrogen-storage systems and batteries utilizing light element (Li, S, etc.).

2.5.3 Dynamics of soft matter and complex fluids

Soft matter and complex fluids cover a spectrum from simple to advanced materials, impacting almost all foods, cosmetics, plastics, films, rubbers, and medical and biomedical materials. These materials are characterized by complexity, flexibility, structural relaxation and non-equilibrium dynamics. The fabrication and processing of such materials, either self-organized or driven, takes place far from equilibrium. Understanding how to control far-from-equilibrium phenomena like jamming, aging, and plastic deformations under stress – to name a few - are important steps needed to achieve breakthrough applications in nanotechnology, material science, and biotechnology [53].

Unfortunately, few tools exist to measure the large ranges of time- and length-scale these materials exhibit. For example, many types of rubber, especially those used to make vehicular tires, use nanoparticles to reinforce mechanical and dynamical viscoelastic properties. Scientists do not yet know what causes these improvements. Better engineered tire

performance requires understanding dynamic behaviors of nanoparticles over enormously disparate time scales; rolling resistance dominates fuel efficiency of vehicles and results during wheel rotation and flexure at ~10 Hz., whereas propulsion and braking use traction and frictional forces at individual contact points occurring at 10^4 to 10^6 Hz (Fig. 8).

ERLs dramatically improve XPCS capabilities to visualize dynamical heterogeneities, dissipative mesoscale fluctuations, and advective responses to shear in non-equilibrium fluids [54]. With a 100-fold increase in coherent flux, ERLs allow measuring time scales 10^4 times faster and make possible numerous experiments that today are beyond reach. The origins of many materials properties in soft matter and complex fluids result from molecular-scale fluctuations on length

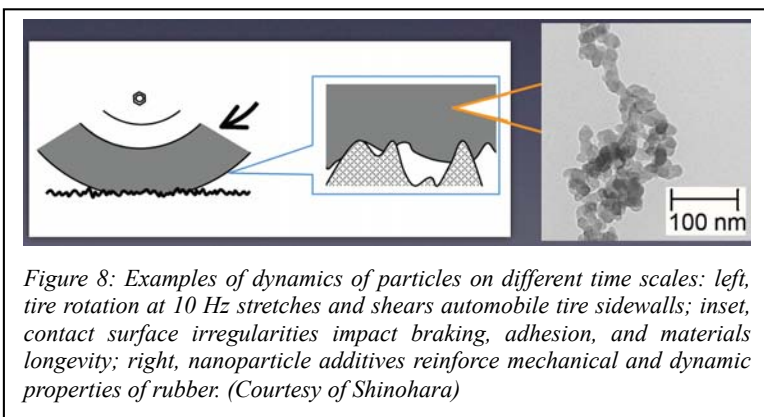


Figure 8: Examples of dynamics of particles on different time scales: left, tire rotation at 10 Hz stretches and shears automobile tire sidewalls; inset, contact surface irregularities impact braking, adhesion, and materials longevity; right, nanoparticle additives reinforce mechanical and dynamic properties of rubber. (Courtesy of Shinohara)

scales from 10-1000 nm and 10^{-6} - 10^{-2} second time scales. XPCS can directly measure these fluctuations, but extracting useful information from most materials on these length and time scales requires 2-3 orders of magnitude more coherent flux increase from an ERL to be practical.

2.6 Grand Challenge: Imaging and harnessing the nanoscale

Advanced materials lie on the critical path to solving many of society's most pressing problems such as sustainable energy, environmental remediation and health. In seeking solutions, scientists need to control and fabricate structures on many different length scales, from the atomic, through nano, to micron and macroscopic scales. Increasingly, scientists and engineers want to build materials that have directed functionalities, for instance mimicking the ability of enzymes in biological systems to build ever more complicated structures to accomplish functional goals. As a result, engineered materials will evolve towards ever increasing complexity such as, for example, larger unit cells, more complicated multi-elemental compositions, heterostructures with sub-micrometer dimensions, and structural modifications at the nanoscale. An ERL will bring to bear powerful tools and techniques able to resolve extremely subtle effects. For example, bond-length changes of hundredths of an Angstrom result in large changes in material properties, such as the metal insulator transition in colossal magneto-resistance manganites [55], or low thermal conductivity above room temperature in PbTe that create promising thermoelectric properties [56].

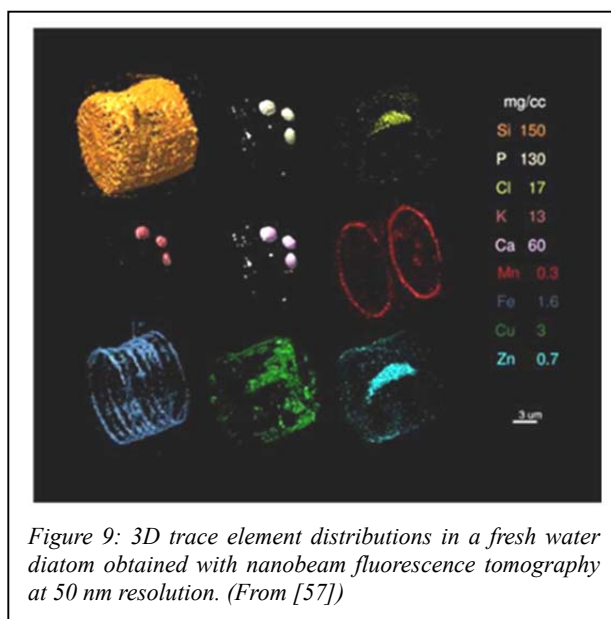


Figure 9: 3D trace element distributions in a fresh water diatom obtained with nanobeam fluorescence tomography at 50 nm resolution. (From [57])

2.6.1 Imaging structure and reactivity of individual nanoparticles

Scientists need to go beyond static structures to probe real materials, *in-situ*, under realistic operating conditions (*in operando*). An ideal X-ray probe would have high intensity, variable beam size (down to a few nanometers), and energy tunability for spectroscopy and diffraction on nano-sized samples embedded in a macroscopic materials. Most importantly, it must be a non-destructive, time resolved probe that can be used to study materials under realistic fabrication, processing and operating conditions.

ERL sources will make nanoprobe tools true workhorse instruments, and extraordinary ERL photon beams will enable fast scanning which, coupled with high-performance detectors, will create new opportunities to obtain 3D information in the time-domain on evolving systems. The "round" beams of ERL sources (both size and divergence) help focusing optics achieve optimal efficiency with superb spatial and angular resolution. Three-dimensional information will become available via tomography techniques [57] (Fig. 9), utilizing absorption and phase contrast, as well as fluorescence and scattering [58] and samples under extreme conditions (i.e. in DACs). ERL coherence can be exploited for coherent imaging [59], where soft tissue studies have been demonstrated on mammography [60] and collagen fibrils [61]. At an ERL such

measurements will be performed in a time-resolved fashion. An ERL will enable ptychographic Bragg coherent diffraction with curved wavefronts, which has the potential to study structure and strain of both isolated and continuous crystalline nanoscale regions in 3D, in complex matrices and *in-situ* [62]. Nanoprobe beamlines on an ERL source will make it routine to combine imaging, spectroscopy, and scattering into a single instrument in order to obtain as complete a suite of information as possible from a single illuminated spot in a specimen.

2.6.2 *Imaging cells and biomembrane dynamics*

Biological materials and systems are true "multi-scale materials" exhibiting complicated structures that evolve with dynamics occurring over a wide range of length and time scales. Studying biomaterials requires exquisite probes of both static structures and dynamics. Dynamics of biological membranes includes, for example, diffusion of lipids and proteins and phonon-like excitations and coherent relaxations, such as undulations, on fast picosecond to nanosecond time scales. Conformational changes of membrane embedded proteins are known to happen on much slower microsecond to millisecond times. Adding to the challenge is growing interest to study structure and dynamics in membrane embedded proteins *in-situ* under physiological conditions.

Visualizing mechanisms of cellular processes and cellular regulation would be an enormous help towards developing strategies for treating disease. Coherent X-ray Diffraction Imaging (CDI) with an ERL has potential to visualize sub-cellular components (e.g. nucleus, chromosomes, Golgi apparatus), in defined functional states, with high, 3D spatial as well as temporal resolution [63] (Fig. 10). While a resolution of 10–15 nm has been achieved [64], resolution is ultimately limited by radiation damage [65]. Using cryopreservation technologies [66-68], the radiation damage can be mitigated,

and a 3D resolution of 5 – 10 nm (or possibly better) might be achieved with the small, bright ERL source. Although CDI has shown potential as a powerful and rapidly developing technique, further development and application has been limited by the availability of intense coherent X-ray sources.

Dynamics at longer length scales involve fluctuations of lipid rafts and nanodomains, and to have relevance to the biological community it is important to study dynamics in water. This leads by necessity to the microsecond regime. XPCS at an ERL source will be the premier tool to study interactions and collective behavior of membrane embedded proteins. With protein-protein distances on the order of 6-10 nanometers, correlated motions will fall into the microsecond XPCS time window. Protein-protein interactions and aggregation could then be studied as a function of membrane composition, such as cholesterol content and protein concentration. Understanding these processes is an extremely important step towards developing a molecular picture of neurodegenerative diseases such as Alzheimer's disease. XPCS, with the 2-3 orders of magnitude increase in brilliance provided by an ERL, may reveal direct signatures of biomembrane domains

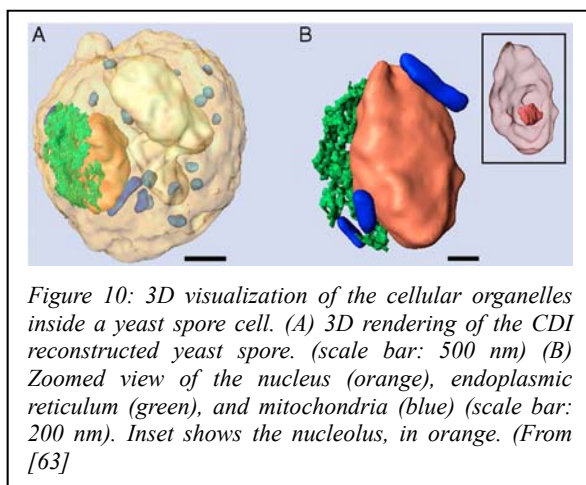


Figure 10: 3D visualization of the cellular organelles inside a yeast spore cell. (A) 3D rendering of the CDI reconstructed yeast spore. (scale bar: 500 nm) (B) Zoomed view of the nucleus (orange), endoplasmic reticulum (green), and mitochondria (blue) (scale bar: 200 nm). Inset shows the nucleolus, in orange. (From [63])

through their fluctuations, which are beyond the reach of other techniques and 3rd generation storage rings, and also not achievable given the time structure from XFELs.

3 ERL Technology Readiness

The principle components of an ERL light source are 1) an injector producing high repetition, ultra-low emittance electron bunches, and 2) a linac using superconducting radio-frequency (SRF) cavities to efficiently accelerate and decelerate bunches to and from high energy. Over the past decade key technologies in each of these major areas have been demonstrated, and extensive additional studies have addressed issues such as beam emittance preservation and suppression of beam-breakup instabilities [7,69]. Energy Recovery has been tested up to 1 GeV at CEBAF [70,71]. Detailed beam optics simulations from front to end of the machine are mature, and all known issues related to emittance growth and beam loss have been studied and can be controlled [7]. The electron beam properties can be adjusted at each undulator (in an ERL light source), thus allowing user stations to adjust the beam properties to their specific needs, something that storage ring system cannot accomplish. There is high confidence that a large-scale ERL can be constructed based on these detailed simulations.

3.1 Photoinjector

Unlike storage ring light sources, where the emission of synchrotron radiation over many recirculations determines the equilibrium emittance and energy spread, the quality of the electron beam produced by an ERL photoinjector can be essentially preserved throughout the machine. Higher electron beam-brightness at the injector translates directly into better X-ray beam quality. The ERL photoinjector must produce reliable beams with low emittance (less than ~20 pm-rad) and moderate current (up to 100 mA) at a high (1300 MHz) repetition rate.

The best electron sources for ERLs all use laser-driven photocathodes. The best performance to date has been achieved at Cornell University using a DC electron gun followed by SRF booster cavities, producing ultra-low emittance beams at energies of 4 MeV and above. As of May 2013, the maximum current delivered was 75 mA. Uninterrupted operation at 65 mA for one day proved a 1/e exponential decay time of nearly 3 days for photocathode efficiency [72]; this performance exceeded the previous record from a photoemission gun by more than a factor of 2 [73]. With the existing laser system, this photoinjector could run continuously for 1 week before replacement (a process taking 15 minutes). This injector already meets the needs of a full-scale ERL hard X-ray light source [74], and if the current beam were accelerated to 5 GeV, the resulting X-ray beam brightness would be about 20 times higher than the brightest today (PETRA-III [75]), and would be close to achieving a fully coherent transverse source.

Photoinjector technology continues to advance rapidly and will push ERL photon beam capabilities even higher. Reducing thermal emittance of the photocathode is a major area of opportunity. In the Cornell photoinjector, photoemission is driven by a high-power fiber laser with sufficient power at 1300 MHz to generate 100 mA from a photocathode with a 1% quantum efficiency (QE) [76]. Current multi-alkali photocathodes have delivered lifetimes that would require less than an hour of downtime each week for replacement. The DC photoemission gun has demonstrated 500 kV operations [73], sufficient to produce ultra-low emittance beams with bunch charges up to 250 pC. Finally, photoinjector simulations, which match the experimental emittance results extremely well, indicate that further R&D advances in photocathode and gun technology will continue to improve X-rays beam performance [7,77].

3.2 Superconducting RF Linac

The SRF linac is a major ERL technology and a cost-driver for both construction and operations. The demands on the liquid helium plant are reduced as cavity fundamental mode quality factor (Q_0) is increased, directly affecting operating budgets for large ERLs. Very high Q_0 has been reached in single-cell cavities and in vertical tests of multi-cell cavities for a number of years. Within the past month, measurements on a fully outfitted 7-cell cavity in a horizontal cryovessel provided spectacular results. At 1.8K a Q_0 of 6×10^{10} was obtained, a factor of three better than specification of 2×10^{10} . A 5 GeV linac constructed from cavities with this performance would require a wall plug power of less than 5 MW, and the total power costs of the facility would be modest compared with other operating costs for a fourth generation source.

3.3 Remaining R&D

While all key ERL technologies have been demonstrated, industrial production of high Q_0 SRF cavities remains. In addition, because energy recovery at the 100 mA level has not been experimentally tested, it would be prudent to test it and validate the SRF cavity design in a small 100 MeV ERL loop. Given the major components for such a loop: the electron gun, the injector Linac, a ERL main Linac cryomodule, and the beam dump, already exist at Cornell, tests could be completed within a few years.

Additional engineering efforts will improve characteristics and reduce costs. In particular, further improvements in photocathodes, which can be replaced at any time, will produce ever-brighter electron and X-ray beams. Likewise, as photoinjector technology improves, a new one can be quickly inserted into the machine. Continued R&D on SRF cavities leading to higher operating Q_0 will push down the yearly operational costs.

In conclusion, the feasibility of an ERL facility is in hand, with only engineering remaining. An ERL facility could be operational in six years after the start of construction.

4 Table 1: Parameters used to compare third and fourth generation X-ray sources

Parameters based on table shown in Reference [41]

		APS	ESRF	Spring8	NSLS II	ERL High Coherence	ERL High Flux
Electron Source	Energy (GeV)	7.0	6.03	8.0	3.0	5.0	5.0
	$\Delta E/E$ (%)	0.096	0.11	0.11	0.099	0.02	0.02
	Current (mA)	100	200	100	500	25	100
	ϵ_N^a (nm·rad)	2.5	4.025	3.4	0.508	0.016 ^a	0.06 ^a
	Coupling	0.00969	0.006	0.002	0.016	1	1
	ϵ_x / ϵ_y (nm·rad)	2.49/0.024	4.0 / 0.024	3.39 / 0.007	0.5 / 0.008	0.008 / 0.008	0.03 / 0.03
	β_x / β_y (m)	14.4 / 4	0.5 / 2.73	21.7 / 14.1	2.02 / 1.06	3.98 / 3.98	3.98 / 3.98
	α_x / α_y	0 / 0	0 / 0	0 / 0	0 / 0	0 / 0	0 / 0
	η_x / η_y (m)	0.124 / 0	0.037 / 0	0.103 / 0	0 / 0	0 / 0	0 / 0
	η'_x / η'_y	0 / 0	0 / 0	0 / 0	0 / 0	0 / 0	0 / 0
	σ_x / σ_y (μm)	224 / 9.82	60.5 / 8.10	294 / 9.78	31.8 / 2.91	5.64 / 5.64	10.9 / 10.9
σ'_x / σ'_y (μrad)	13.2 / 2.46	89.5 / 2.97	12.5 / 0.69	15.7 / 2.75	1.42 / 1.42	2.75 / 2.75	
Undulator / X-ray Source	Type	Undulator A	In vacuum undulator	In vacuum undulator	U20 undulator	Helical Delta	Helical Delta
	Beamline	8ID	ID27	BL19XU	Projected	Projected	Projected
	Length (m)	2.4	4	25	3	25	25
	Period (mm)	33	23	32	20	18	18
	Min. Gap (mm)	10.5	6	12	5	5	5
	B_{max} (T)	0.891	0.75	0.59	0.97	0.85	0.85
	K_{max}	2.74	1.61	1.76	1.81	1.43	1.43
	Σ_x / Σ_y (μm) ^b	224 / 10.1	60.5 / 8.56	294.1 / 12.0	32.1 / 5.11	8.99 / 8.99	13.0 / 13.0
	Σ'_x / Σ'_y (μrad) ^b	14.3 / 6.21	89.6 / 5.31	12.6 / 1.89	18.0 / 9.21	2.26 / 2.26	3.26 / 3.26
	Spectral Brightness ^{bc}	4.2×10^{19}	1.6×10^{20}	6.4×10^{20}	8.9×10^{20}	8.0×10^{22}	8.9×10^{22}
	Coherent Fraction (%) ^b	0.080	0.054	0.085	0.82	24	6.6
Coherent Flux (ph/s/0.1%) ^b	2.5×10^{11}	9.5×10^{11}	3.9×10^{12}	5.4×10^{12}	4.8×10^{14}	5.4×10^{14}	

^a SPECTRA-8.0.10 calculates ϵ_x and ϵ_y based on a “Natural Emittance” parameter (ϵ_N) and the coupling constant, so we have included ϵ_N in this table. Spectra models an isotropic source as having unit coupling, ϵ_N is therefore double that of ϵ_x and ϵ_y . When comparing an ERL with existing sources, ϵ_x and ϵ_y are the relevant parameters, not ϵ_N .

^b Values at 8 keV. Σ , Σ' refer to width and divergence, resp.

^c Spectral Brightness reported in standard units of ph/s/mm²/mrad²/0.1% bw.

Table 1. Parameters used to calculate spectral brightness and coherent flux in figure 1. Values for other sources are good faith estimates based on information posted by the sources on their websites. Nominal values were used where possible to give a fair comparison between existing and projected sources. In the case of NSLS II, the emittances used are for the 8 damping wiggler configuration. All calculations were performed using SPECTRA-8.0.10.

5 References

- [1] "Next-Generation Photon Sources for Grand Challenges in Science and Energy: Report of the Workshop on Solving Science and Energy Grand Challenges with Next-Generation Photon Sources," 2008, see http://science.energy.gov/~media/bes/pdf/reports/files/ngps_rpt.pdf.
- [2] DESY, "Brilliant future for PETRA III," CERN Courier **43** (6), 7 (2003).
- [3] A. Ropert, Filhol, J.M., Elleaume, P., Farvacque, L., Hardy, L, Jacob, J., Weinrich, U., "Towards the ultimate storage ring-based light source," Proc. EPAC 2000, 83.
- [4] Martin Magnuson, Mats Fahlman, Roger Uhrberg, Leif Johansson, and - Total of 100 authors in alphabetical orders, "MAX IV Conceptual Design Report (CDR)," 2006, see <http://urn.kb.se/resolve?urn=urn:nbn:se:liu:diva-60634>.
- [5] "Energy Recovery Linac Preliminary Design Report (KEK)," 2012, see http://pfwww.kek.jp/ERLoffice/detabase/ERL%20Preliminary%20Design%20Report_web.pdf.
- [6] M. Borland, presented at the Particle Accelerator Conference (PAC09), 2009, MO3PBI01 (unpublished).
- [7] G. Hoffstaetter, S. M. Gruner, and M. Tigner (editors); A. Bartnik, I. V. Bazarov, D. H. Bilderback, M. G. Billing, J. D. Brock, J. A. Crittenden, L. Cultrera, D. Dale, J. A. Dobbins, B. M. Dunham, R. D. Ehrlich, M. P. Ehrlichman, R. Eichhorn, K. D. Finkelstein, E. Fontes, M. J. Forster, S. Full, F. Furuta, D. Gonnella, S. W. Gray, S. M. Gruner, C. Gulliford, D. L. Hartill, Y. He, R. G. Helmke, V. Ho, R. P. Kaplan, S. S. Karkare, V. O. Kostroun, H. A. Lee, Y. Li, X. Liu, M. U. Liepe, C. E. Mayes, J. M. Maxson, A. A. Mikhailichenko, H. S. Padamsee, R. Patterson, S. B. Peck, S. E. Posen, P. G. Quigley, P. Revesz, D. H. Rice, D. C. Sagan, J. O. Sears, V. D. Shemelin, D. M. Smilgies, E. N. Smith, K. W. Smolenski, A. B. Temnykh, M. Tigner, N. R. A. Valles, V. G. Veshcherevich, A. R. Woll, Y. Xie, Z. Zhao, "Cornell Energy Recovery Linac Project Definition Design Report (PDDR)," 2013, see <http://erl.chess.cornell.edu/PDDR/PDDR.pdf>.
- [8] K. D. Finkelstein, I. V. Bazarov, A. Liepe, Q. Shen, D. Bilderback, S. Gruner, and A. Kazimirov, "Energy recovery LINAC: A next generation source for inelastic X-ray scattering," Journal of Physics and Chemistry of Solids **66** (12), 2310-2312 (2005).
- [9] Donald H. Bilderback, Joel D. Brock, Darren S. Dale, Kenneth D. Finkelstein, Mark A. Pfeifer, and Sol M. Gruner, "Energy recovery linac (ERL) coherent hard x-ray sources," New Journal of Physics **12** (3), 035011 (2010).
- [10] K. J. Kim, Y. Shvyd'ko, and S. Reiche, "A proposal for an x-ray free-electron laser oscillator with an energy-recovery linac," Physical Review Letters **100** (24), 244802 (2008).
- [11] Kwang-Je Kim and Yuri V. Shvyd'ko, "Tunable optical cavity for an x-ray free-electron-laser oscillator," Physical Review Special Topics - Accelerators and Beams **12** (3), 030703 (2009).
- [12] M. Tigner, "A Possible Apparatus for Electron Clashing-Beam Experiments," Nuovo Cimento **37** (3), 1228-1231 (1965).
- [13] M. Borland, G. Decker, A. Nassiri, Y. E. Sun, and M. White, "Potential performance and challenges of an energy recovery linac upgrade to the Advanced Photon Source," Nuclear Instruments & Methods in Physics Research Section a-Accelerators Spectrometers Detectors and Associated Equipment **582** (1), 54-56 (2007).
- [14] J. Bisognano, "Future SRF-linac based light sources: initiatives and issues," SRF-2009. <http://accelconf.web.cern.ch/AccelConf/srf2009/papers/frobau01.pdf> (2009).
- [15] E. Fontes, "Cornell ERL Prototype Successes Grow," 2012, see <http://news.chess.cornell.edu/articles/2012/ERLgoals02152012.html>.
- [16] E. Fontes, "Cornell Surpasses Milestones Towards New ERL Coherent X-ray Source," 2011, see <http://news.chess.cornell.edu/articles/2011/CoherentOct2011.html>.

- [17] Cornell ERL Workshops, "X-ray Science Opportunities with an ERL, series of six international workshops at Cornell University, Cornell University, June 5-24, 2006.," 2006, see <http://erl.chess.cornell.edu/gatherings/erl%20workshop/index.htm>.
- [18] D. Dale, S. M. Gruner, J. Brock, D. Bilderback, and E. Fontes, "Science at the Hard X-ray Diffraction Limit (XDL2011), Part 1," *Synchrotron Radiation News* **24**, 4-11 (2012).
- [19] Zhongwu Wang, Ken Finkelstein, Detlef Smilgies, Arthur Woll, and Ernie Fontes, "Science at the Hard X-ray Diffraction Limit (XDL2011), Part 2," *Synchrotron Radiation News* **25** (1), 9-16 (2012).
- [20] D.H. Bilderback, J.D. Brock, E. Fontes, G.H. Hoffstaetter (editors), and others, "Science with an Energy Recovery Linac (ERL)," 2013, see http://www.classe.cornell.edu/ERL/Images/Science_with_an_ERL.pdf.
- [21] Svetlana S. van Bavel, Erwan Sourty, Gijsbertus de With, and Joachim Loos, "Three-Dimensional Nanoscale Organization of Bulk Heterojunction Polymer Solar Cells," *Nano Letters* **9** (2), 507-513 (2008).
- [22] Maryana Escalante, Aufried Lenferink, Yiping Zhao, Niels Tas, Jurriaan Huskens, C. Neil Hunter, Vinod Subramaniam, and Cees Otto, "Long-Range Energy Propagation in Nanometer Arrays of Light Harvesting Antenna Complexes," *Nano Letters* **10** (4), 1450-1457 (2010).
- [23] G. Vanko, P. Glatzel, V. T. Pham, R. Abela, D. Grolimund, C. N. Borca, S. L. Johnson, C. J. Milne, and C. Bressler, "Picosecond Time-Resolved X-Ray Emission Spectroscopy: Ultrafast Spin-State Determination in an Iron Complex," *Angewandte Chemie-International Edition* **49** (34), 5910-5912 (2010).
- [24] P. W. Anderson, "More Is Different," *Science* **177** (4047), 393-396 (1972).
- [25] A.B. Temnykh, "Delta Undulator for Cornell Energy Recovery Linac," *Phys. Rev. St Accel Beams* **11**, 120702 (2008).
- [26] E. Dagotto, "Complexity in strongly correlated electronic systems," *Science* **309** (5732), 257-262 (2005).
- [27] M. Uehara, S. Mori, C. H. Chen, and S. W. Cheong, "Percolative phase separation underlies colossal magnetoresistance in mixed-valent manganites," *Nature* **399** (6736), 560-563 (1999).
- [28] E. Dagotto, J. Burgy, and A. Moreo, "Nanoscale phase separation in colossal magnetoresistance materials: lessons for the cuprates?," *Solid State Communications* **126** (1-2), 9-22 (2003).
- [29] J. Lee, K. Fujita, K. McElroy, J. A. Slezak, M. Wang, Y. Aiura, H. Bando, M. Ishikado, T. Masui, J. X. Zhu, A. V. Balatsky, H. Eisaki, S. Uchida, and J. C. Davis, "Interplay of electron-lattice interactions and superconductivity in $\text{Bi}_2\text{Sr}_2\text{CaCu}_2\text{O}_{8+\delta}$," *Nature* **442** (7102), 546-550 (2006).
- [30] K. K. Gomes, A. N. Pasupathy, A. Pushp, S. Ono, Y. Ando, and A. Yazdani, "Visualizing pair formation on the atomic scale in the high-T-c superconductor $\text{Bi}_2\text{Sr}_2\text{CaCu}_2\text{O}_{8+\delta}$," *Nature* **447** (7144), 569-572 (2007).
- [31] M. Vershinin, S. Misra, S. Ono, Y. Abe, Y. Ando, and A. Yazdani, "Local ordering in the pseudogap state of the high-T-c superconductor $\text{Bi}_2\text{Sr}_2\text{CaCu}_2\text{O}_{8+\delta}$," *Science* **303** (5666), 1995-1998 (2004).
- [32] M. M. Qazilbash, A. Tripathi, A. A. Schafgans, B. J. Kim, H. T. Kim, Z. H. Cai, M. V. Holt, J. M. Maser, F. Keilmann, O. G. Shpyrko, and D. N. Basov, "Nanoscale imaging of the electronic and structural transitions in vanadium dioxide," *Physical Review B* **83** (16), 165108-165125 (2011).
- [33] Tingting Qi, Young-Han Shin, Ka-Lo Yeh, Keith A. Nelson, and Andrew M. Rappe, "Collective Coherent Control: Synchronization of Polarization in Ferroelectric PbTiO_3 by Shaped THz Fields," *Physical Review Letters* **102** (24), 247603 (2009).
- [34] S. Eisebitt, J. Luning, W. F. Schlotter, M. Lorgen, O. Hellwig, W. Eberhardt, and J. Stohr, "Lensless imaging of magnetic nanostructures by X-ray spectro-holography," *Nature* **432** (7019), 885-888 (2004).
- [35] I. McNulty, J. Kirz, C. Jacobsen, E. H. Anderson, M. R. Howells, and D. P. Kern, "High-Resolution

- Imaging by Fourier-Transform X-Ray Holography," *Science* **256** (5059), 1009-1012 (1992).
- [36] S. Marchesini, S. Boutet, A. E. Sakdinawat, M. J. Bogan, S. Bajt, A. Barty, H. N. Chapman, M. Frank, S. P. Hau-Riege, A. Szoke, C. W. Cui, D. A. Shapiro, M. R. Howells, J. C. H. Spence, J. W. Shaevitz, J. Y. Lee, J. Hajdu, and M. M. Seibert, "Massively parallel X-ray holography," *Nature Photonics* **2** (9), 560-563 (2008).
- [37] Jianwei Miao, Pambos Charalambous, Janos Kirz, and David Sayre, "Extending the methodology of X-ray crystallography to allow imaging of micrometre-sized non-crystalline specimens," *Nature* **400** (6742), 342-344 (1999).
- [38] I. Robinson and R. Harder, "Coherent X-ray diffraction imaging of strain at the nanoscale," *Nature Materials* **8** (4), 291-298 (2009).
- [39] D. Shapiro, P. Thibault, T. Beetz, V. Elser, M. Howells, C. Jacobsen, J. Kirz, E. Lima, H. Miao, A. M. Neiman, and D. Sayre, "Biological imaging by soft X-ray diffraction microscopy," *Proceedings of The National Academy of Sciences of the United States of America* **102** (43), 15343-15346 (2005).
- [40] J. M. Rodenburg, A. C. Hurst, A. G. Cullis, B. R. Dobson, F. Pfeiffer, O. Bunk, C. David, K. Jefimovs, and I. Johnson, "Hard-x-ray lensless imaging of extended objects," *Phys Rev Lett* **98** (3), 034801 (2007).
- [41] D. H. Bilderback, J. D. Brock, D. S. Dale, K. D. Finkelstein, M. A. Pfeifer, and S. M. Gruner, "Energy recovery linac (ERL) coherent hard x-ray sources," *New Journal of Physics* **12** (2010).
- [42] P. Thibault, V. Elser, C. Jacobsen, D. Shapiro, and D. Sayre, "Reconstruction of a yeast cell from X-ray diffraction data," *Acta Crystallographica Section A* **62**, 248-261 (2006).
- [43] Ian Robinson and Ross Harder, "Coherent X-ray diffraction imaging of strain at the nanoscale," *Nat Mater* **8** (4), 291-298 (2009).
- [44] M.P. Miller, R. M. Suter, U. Lienert, A.J. Beaudoin, E. Fontes, J. Almer, and J.C. Schuren, "High-energy Needs and Capabilities to Study Multiscale Phenomena in Crystalline Materials," *Synchrotron Radiation News* **25** (6), 18 (2012).
- [45] M. C. Newton, S. J. Leake, R. Harder, and I. K. Robinson, "Three-dimensional imaging of strain in a single ZnO nanorod," *Nature Materials* **9** (2), 120-124 (2010).
- [46] W. Ludwig, P. Reischig, A. King, M. Herbig, E. M. Lauridsen, G. Johnson, T. J. Marrow, and J. Y. Buffiere, "Three-dimensional grain mapping by x-ray diffraction contrast tomography and the use of Friedel pairs in diffraction data analysis," *Review of Scientific Instruments* **80** (3) (2009).
- [47] S. F. Li and R. M. Suter, "Adaptive Reconstruction Method for Three-Dimensional Orientation Imaging," *Journal of Applied Crystallography* **46**, 512-524 (2013).
- [48] J. L. Flament, F. Zielinski, S. Saude, and R. I. Grynszpan, "Helium diffusion in metals investigated by nuclear reaction analysis," *Nuclear Instruments & Methods in Physics Research Section B-Beam Interactions with Materials and Atoms* **216**, 161-166 (2004).
- [49] J. W. M. Frenken, B. J. Hinch, and J. P. Toennies, "He Scattering Study of Diffusion at a Melting Surface," *Surface Science* **211** (1-3), 21-30 (1989).
- [50] R. Lewis and R. Gomer, "Adsorption Studies with Field Ion Microscope - Phys," *Abstracts of Papers of the American Chemical Society (Sep)*, 6-14 (1970).
- [51] F. E. Wagner, R. Wordel, and M. Zelger, "Influence of Interstitial Diffusion on the Mossbauer-Spectra of Iron Solutes in Vd0.78 and Nbh0.84," *Journal of Physics F-Metal Physics* **14** (2), 535-547 (1984).
- [52] M. Leitner, B. Sepiol, L. M. Stadler, B. Pfau, and G. Vogl, "Atomic diffusion studied with coherent X-rays," *Nat Mater* **8** (9), 717-720 (2009).
- [53] Bernd Struth, Kyu Hyun, Efim Kats, Thomas Meins, Michael Walther, Manfred Wilhelm, and Gerhard Grübel, "Observation of New States of Liquid Crystal 8CB under Nonlinear Shear Conditions as Observed via a Novel and Unique Rheology/Small-Angle X-ray Scattering

- Combination," *Langmuir* **27** (6), 2880-2887 (2011).
- [54] A. Fluerasu, P. Kwasniewski, C. Caronna, F. Destremaut, J. B. Salmon, and A. Madsen, "Dynamics and rheology under continuous shear flow studied by x-ray photon correlation spectroscopy," *New Journal of Physics* **12**, 035023-035033 (2010).
- [55] S. J. Billinge, R. G. DiFrancesco, G. H. Kwei, J. J. Neumeier, and J. D. Thompson, "Direct Observation of Lattice Polaron Formation in the Local Structure of $\text{La}_{1-x}\text{Ca}_x\text{MnO}_3$," *Phys Rev Lett* **77** (4), 715-718 (1996).
- [56] E. S. Bozin, C. D. Malliakas, P. Souvatzis, T. Proffen, N. A. Spaldin, M. G. Kanatzidis, and S. J. Billinge, "Entropically stabilized local dipole formation in lead chalcogenides," *Science* **330** (6011), 1660-1663 (2010).
- [57] M. D. de Jonge and S. Vogt, "Hard X-ray fluorescence tomography--an emerging tool for structural visualization," *Curr Opin Struct Biol* **20** (5), 606-614 (2010).
- [58] M. Kuhlmann, J. M. Feldkamp, J. Patommel, S. V. Roth, A. Timmann, R. Gehrke, P. Muller-Buschbaum, and C. G. Schroer, "Grazing Incidence Small-Angle X-ray Scattering Microtomography Demonstrated on a Self-Ordered Dried Drop of Nanoparticles," *Langmuir* **25** (13), 7241-7243 (2009).
- [59] C. G. Schroer, R. Boye, J. M. Feldkamp, J. Patommel, A. Schropp, A. Schwab, S. Stephan, M. Burghammer, S. Schoder, and C. Riekel, "Coherent x-ray diffraction imaging with nanofocused illumination," *Physical Review Letters* **101** (9), 090801-090805 (2008).
- [60] X. Wu, H. Liu, and A. Yan, "X-ray phase-attenuation duality and phase retrieval," *Optics Letters* **30** (4), 379-381 (2005).
- [61] F. Berenguer de la Cuesta, M. P. Wenger, R. J. Bean, L. Bozec, M. A. Horton, and I. K. Robinson, "Coherent X-ray diffraction from collagenous soft tissues," *Proc Natl Acad Sci U S A* **106** (36), 15297-15301 (2009).
- [62] Stephan O. Hruszkewycz, Martin V. Holt, Ash Tripathi, Jörg Maser, and Paul H. Fuoss, "Framework for three-dimensional coherent diffraction imaging by focused beam x-ray Bragg ptychography," *Opt. Lett.* **36** (12), 2227-2229 (2011).
- [63] H. D. Jiang, C. Y. Song, C. C. Chen, R. Xu, K. S. Raines, B. P. Fahimian, C. H. Lu, T. K. Lee, A. Nakashima, J. Urano, T. Ishikawa, F. Tamanoi, and J. W. Miao, "Quantitative 3D imaging of whole, unstained cells by using X-ray diffraction microscopy," *Proceedings of The National Academy of Sciences of the United States of America* **107** (25), 11234-11239 (2010).
- [64] J. Nelson, X. J. Huang, J. Steinbrener, D. Shapiro, J. Kirz, S. Marchesini, A. M. Neiman, J. J. Turner, and C. Jacobsen, "High-resolution x-ray diffraction microscopy of specifically labeled yeast cells," *Proceedings of The National Academy of Sciences of the United States of America* **107** (16), 7235-7239 (2010).
- [65] M. R. Howells, T. Beetz, H. N. Chapman, C. Cui, J. M. Holton, C. J. Jacobsen, J. Kirz, E. Lima, S. Marchesini, H. Miao, D. Sayre, D. A. Shapiro, J. C. H. Spence, and D. Starodub, "An assessment of the resolution limitation due to radiation-damage in X-ray diffraction microscopy," *Journal of Electron Spectroscopy and Related Phenomena* **170** (1-3), 4-12 (2009).
- [66] X. J. Huang, J. Nelson, J. Kirz, E. Lima, S. Marchesini, H. J. Miao, A. M. Neiman, D. Shapiro, J. Steinbrener, A. Stewart, J. J. Turner, and C. Jacobsen, "Soft X-Ray Diffraction Microscopy of a Frozen Hydrated Yeast Cell," *Physical Review Letters* **103** (19) (2009).
- [67] E. Lima, L. Wiegart, P. Pernot, M. Howells, J. Timmins, F. Zontone, and A. Madsen, "Cryogenic X-Ray Diffraction Microscopy for Biological Samples," *Physical Review Letters* **103** (19) (2009).
- [68] C. U. Kim, J. L. Wierman, R. Gillilan, E. Lima, and S. M. Gruner, "A high-pressure cryocooling method for protein crystals and biological samples with reduced background X-ray scatter," *Journal of Applied Crystallography* **46** (1), 234-241 (2013).
- [69] Adam Bartnik Colwyn Gulliford, Ivan Bazarov, Luca Cultrera, John Dobbins, Bruce Dunham,

- Francisco Gonzalez, Georg Hoffstaetter, Siddharth Karkare, Hyeri Lee, Heng Li, Yulin Li, Xianghong Liu, Jared Maxson, Christian Nguyen, Karl Smolenski, Zhi Zhao, "Demonstration of Low Emittance in the Cornell Energy Recovery Linac Injector Prototype," arXiv.org **arXiv:1304.2708** (2013).
- [70] A. P. Freyberger, K. Beard, A. Bogacz, Y. Chao, S. Chattopadhyay, D. Douglas, A. Hutton, L. Merminga, C. Tennant, and M. Tiefenback, "The CEBAF energy recovery experiment: Update and future plans," Proceedings EPAC04 (2004) (2004).
- [71] A. Bogacz, K. Beard, J. Bengtsson, C. Butler, Y. Chao, S. Chattopadhyay, H. Dong, D. Douglas, A. Freyberger, A. Guerra, R. Hicks, A. Hofler, C. Hovater, A. Hutton, R. Kazimi, R. Lauze, L. Merminga, T. Plawski, Y. Roblin, M. Spata, C. Tennant, M. Tiefenback, A. Bernhard, A. Magerl, H. Toyokawa, "CEBAF Energy Recovery Experiment," Proceedings of the 2003 Particle Accelerator Conference (2003).
- [72] S. Karkare, L. Cultrera, B. Lillard, A. Bartnik, I. Bazarov, B. Dunham, W. Schaff, K. Smolenski, "Growth and characterization of rugged Sodium Potassium Antimonide photocathodes for high brilliance photoinjector," Applied Physics Letters (Submitted) (2013).
- [73] Bruce Dunham, John Barley, Adam Bartnik, Ivan Bazarov, Luca Cultrera, John Dobbins, Georg Hoffstaetter, Brent Johnson, Roger Kaplan, Siddharth Karkare, Vaclav Kostroun, Yulin Li, Matthias Liepe, Xianghong Liu, Florian Loehl, Jared Maxson, Peter Quigley, John Reilly, David Rice, Daniel Sabol, Eric Smith, Karl Smolenski, Maury Tigner, Vadim Vesherevich, Dwight Widger, and Zhi Zhao, "Record high-average current from a high-brightness photoinjector," Applied Physics Letters **102** (3), 034105-034104 (2013).
- [74] A. Bartnik, G. Hoffstaetter, I. Bazarov, D. Bilderback, M. Billing, J. Brock, J. Crittenden, L. Cultrera, D. Dale, J. Dobbins, B. Dunham, R. Ehrlich, M. Ehrlichman, R. Eichhorn, K. Finkelstein, E. Fontes, M. Forster, S. Full, F. Furuta, D. Gonnella, S. Gray, S. Gruner, C. Gulliford, D. Hartill, Y. He, R. Helmke, K. Ho, R. Kaplan, S. Karkare, V. Kostroun, H. Lee, Y. Li, M. Liepe, X. Liu, J. Maxson, C. Mayes, A. Mikhailichenko, H. Padamsee, J. Patterson, S. Peck, S. Posen, P. Quigley, P. Revesz, D. Rice, D. Sagan, J. Sears, V. Shemelin, D. Smilgies, E. Smith, K. Smolenski, A. Temnykh, M. Tigner, N. Valles, V. Veshcherevich, A. Woll, Y. Xie, Z. Zhao, presented at the Fourth International Particle Accelerator Conference (IPAC13), Shanghai, China, 2013 (unpublished).
- [75] M. Bieler, K. Balewski, J. Keil, A. Kling, G. Sahoo, R. Wanzenberg, presented at the International Particle Accelerator Conference (IPAC2011), San Sebastián, Spain, 2011 (unpublished).
- [76] Z. Zhao, B. M. Dunham, I. Bazarov, and F. W. Wise, "Generation of 110 W infrared and 65 W green power from a 1.3-GHz sub-picosecond fiber amplifier," Optics Express **20** (5), 4850-4855 (2012).
- [77] H. Li, I. V. Bazarov, B. M. Dunham, and F. W. Wise, "Three-dimensional laser pulse intensity diagnostic for photoinjectors," Physical Review Special Topics-Accelerators and Beams **14** (11) (2011).